# Image enhancement for pattern recognition

Quyen Huynh[a,b], Nicola Neretti[a], Nathan Intrator[a], and Gerry Dobeck[b]

[a]Institute for Brain and Neural System, Brown University, Providence, RI 02912
[b]Coastal Systems Station, Naval Surface Warfare Center, Panama City, FL 32407-7001

## ABSTRACT

We investigate various image enhancement techniques geared towards a specific detector. Our database consists of side-scan sonar images collected at the Naval Surface Warfare Center (NSWC), and the detector we use has proven to have excellent results on these data. We start by investigating various wavelet and wavelet packet denoising methods. Other methods we consider are based on more common filters (gaussian and DOG filters). In wavelet based denoising we try different approaches, combining techniques that have been succesfully used in signal and image denoising. We notice that the performance is mostly affected by the choice of the scale levels to which shrinkage is applied. We demonstrate that wavelet denoising can significantly improve detection performance while keeping low false alarm rates.

**Keywords:** Image processing, Wavelets, Pattern recognition

## 1. METHODOLOGY

Discrimination problems differ in nature from reconstruction tasks. While in reconstruction, it is the mean squared error that is often used to measure the quality of the scheme, classification requires a different measure which often is not related to the former. The discrimination power of a certain basis or a set of basis function is not necessarily connected to the quality of reconstruction associated with this set.

As part of our effort to construct an integrated system for mine detection, we started investigating various image enhancement techniques which are geared towards a specific detector* that has proven to have excellent results on this data. We started by investigating various wavelet and wavelet packet denoising methods.

Other methods that we have considered are based on more common filters. In particular we used a Gaussian filter with $\sigma = 2$, and a DOG filter (Difference Of Gaussians) with $\sigma_1 = 1$ and $\sigma_2 = 3$. Their parameters have been chosen so as not to smear the difference between the highlight of the mine and its shadow.

In the wavelet based denoising we used two different approaches. The first one is the direct application of Donoho's shrinkage[1]. It consists of choosing a certain level in the wavelet representation, which we suspect, contains noise that could affect the detection, and then shrinking its coefficients. We considered two types of mother wavelets: Coiflet-5 and Symmlet-8. It is also possible to shrink at different levels and even shrink with different mother wavelets based on a careful examination of the signal. Following Coifman and Majid[2], we first shrinked the coefficients at a certain level and then shrinked again at a different level the denoised (reconstructed) image from the first level. Again, we used Coiflet-5 and Symmlet-8 mother wavelets. The scales for shrinkage were chooses so as to fit approximately the mine-like targets dimension. It turned out that a good choice would include levels between the first and the third, the first level corresponding to the finest scale.

## 2. DESCRIPTION OF DATA

The data base we used consists of a 60-image set from a side-scan sonar (SSS0) collected at the Naval Surface Warfare Center (NSWC). They are encoded as 8-bit gray scale images, 1024 range cells by 511 cross-range cells. The 60 images contain 33 targets; some contain more than one target while others contain no targets. Non-target objects which look as targets appear throughout the images. A typical mine-like target consists

*Constructed by Dr. John Hyland and Dr. Gerry Dobeck from NSWC.

Performance summary

| Type of image preprocessing | Pd (%) | FA/Image |
|---|---|---|
| Original | 91 | 1.17 |
| Original | 97 | 3.8 |
| Gaussian | 91 | 1.57 |
| Coiflet-5 (1st level) | 97 | 1.38 |
| Symmlet-8 (1st level) | 97 | 1.37 |
| Coiflet-5 (2nd level) | 91 | 0.9 |
| Coiflet-5 (2nd level) | 97 | 1.20 |
| Symmlet-8 (2nd level) | 97 | 1.22 |
| Coiflet-5 (1st level), Symmlet-8 (2nd level) | 97 | 1.37 |
| Coiflet-5 (1st level), Symmlet-8 (2nd level), Coiflet-5 (3rd level) | 97 | 1.28 |

Table 1: Performance of the detection stage of the AMDAC algorithm for different denoising techniques. Percent correct classification is followed by the average number of false alarms per image.

of a strong highlight on its left side and a long shadow down range on its right side. Unfortunately the presence of clutter can mask this structure. This is clearly seen in Figure 1 which contains one of the files used in this study.

Real sonar image data is preferred over simulated sonar data because sonar simulations are expensive and do not capture all the critical dynamics associated with actual sonar images.

## 3. FREQUENCY RESPONSE

To get some intuition about the effect of the denoising methods, we analyzed their frequency response before and after denoising. Figures 2 and 3 depict the Fourier transform of an original image (top), and of the same image denoised with different denoising techniques (center and bottom). We note the presence of very high values in the low frequency domain in the original images. A possible interpretation is the presence of regular periodic structures (sand waves on the sea bottom, trails created by fish nets) and a correlation between pixels due to the slow movement of the sonar detector. The wavelet denoising had little effect on these low frequencies. The DOG filter has a stronger effect as it behaves more like a bandpass and thus, decreases both the high and low frequency response. This behavior is better seen in the histogram of the frequency response (Figure 4) where one can see the distortion to the histogram caused by the DOG and Gaussian filters vs. the distortion caused by the wavelet denoising methods.

## 4. HYBRID CLASSIFICATION SCHEME

To test the effectiveness of the denoising method, we employed it in a full detection and classification scheme. We used the detection stage of the current best scheme – the Advanced Mine Detection and Classification (AMDAC) algorithm developed at the Naval Surface Warfare Center (NSWC)[3]. This scheme is a combination of a detection density algorithm applied to a non-linear matched filter response and followed by a classification feature extractor and a k-nearest neighbor (KNN) classifier.

We chose to concentrate on the detection stage since it is considered to be the most critical; Its purpose is to scan the entire image and identify candidate mine-like regions that will be more thoroughly analyzed by the subsequent classification stages. If a mine-like region is not detected at this stage it will not be possible to recover it afterwards.

## 5. MATCHED FILTER

The matched filter is designed to detect a mine-like structure, a highlight with the shadow behind it (Figure 5). Relying on the existence of a shadow can dramatically reduce the false positive response of the detector. The challenge to a successful denoising method is to preserve this sharp distinction between mine

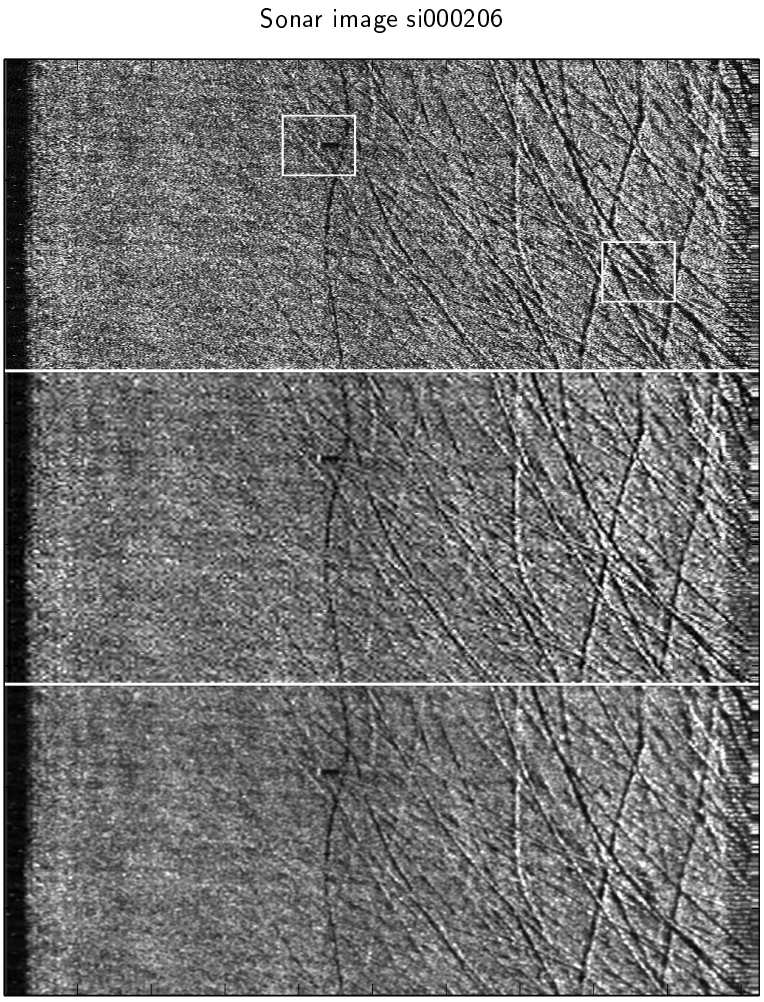


Figure 1: Original image (top), wavelet denoised image (center), and Gaussian filtered image (bottom). Mine-like objects in the original image have been enclosed in white squares.

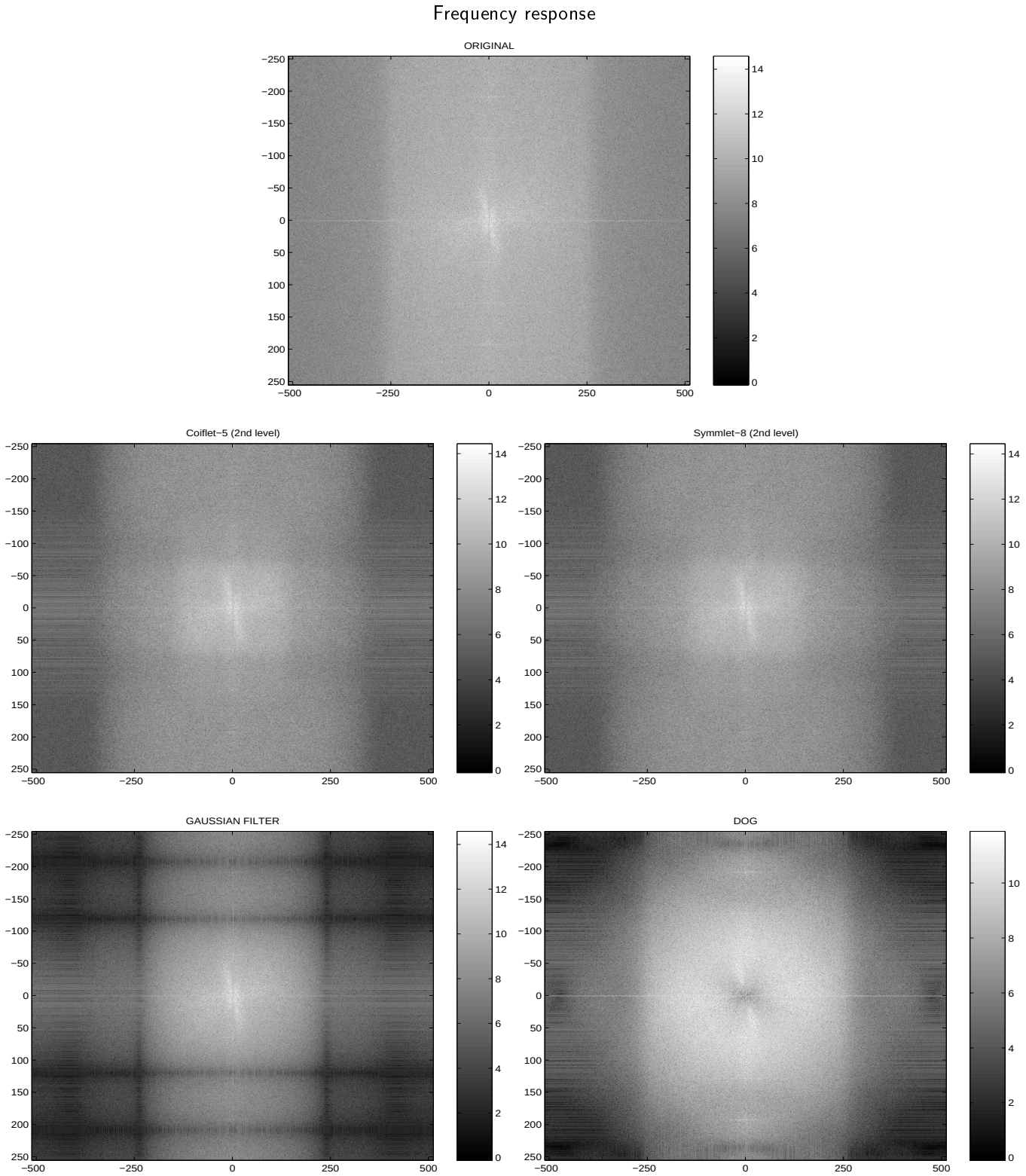


Figure 2: Fourier transform of the original image (top), and of the same image denoised with different denoising techniques (center and bottom).

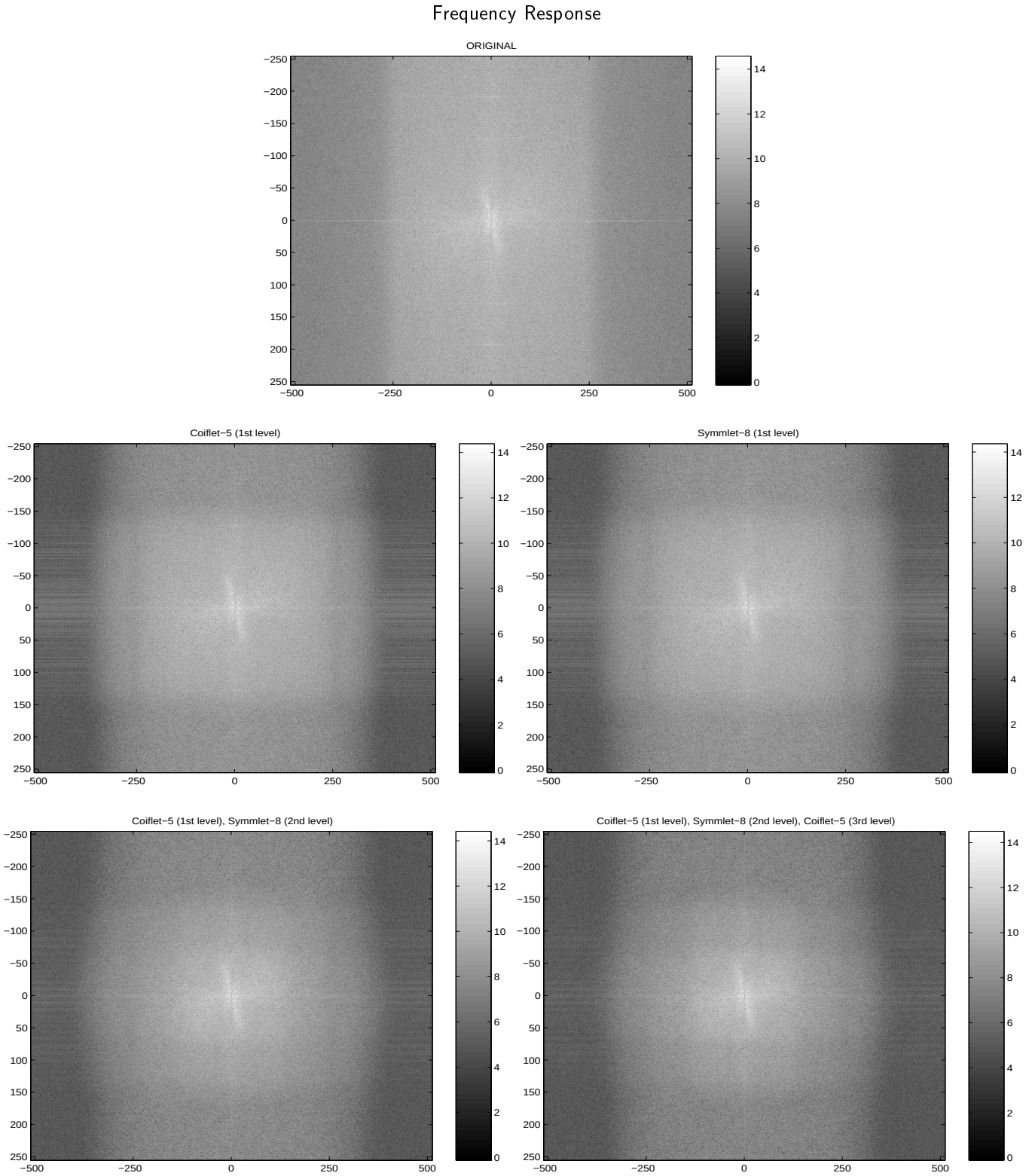


Figure 3: Fourier transform of the original image (top), and of the same image denoised with different denoising techniques (center and bottom).

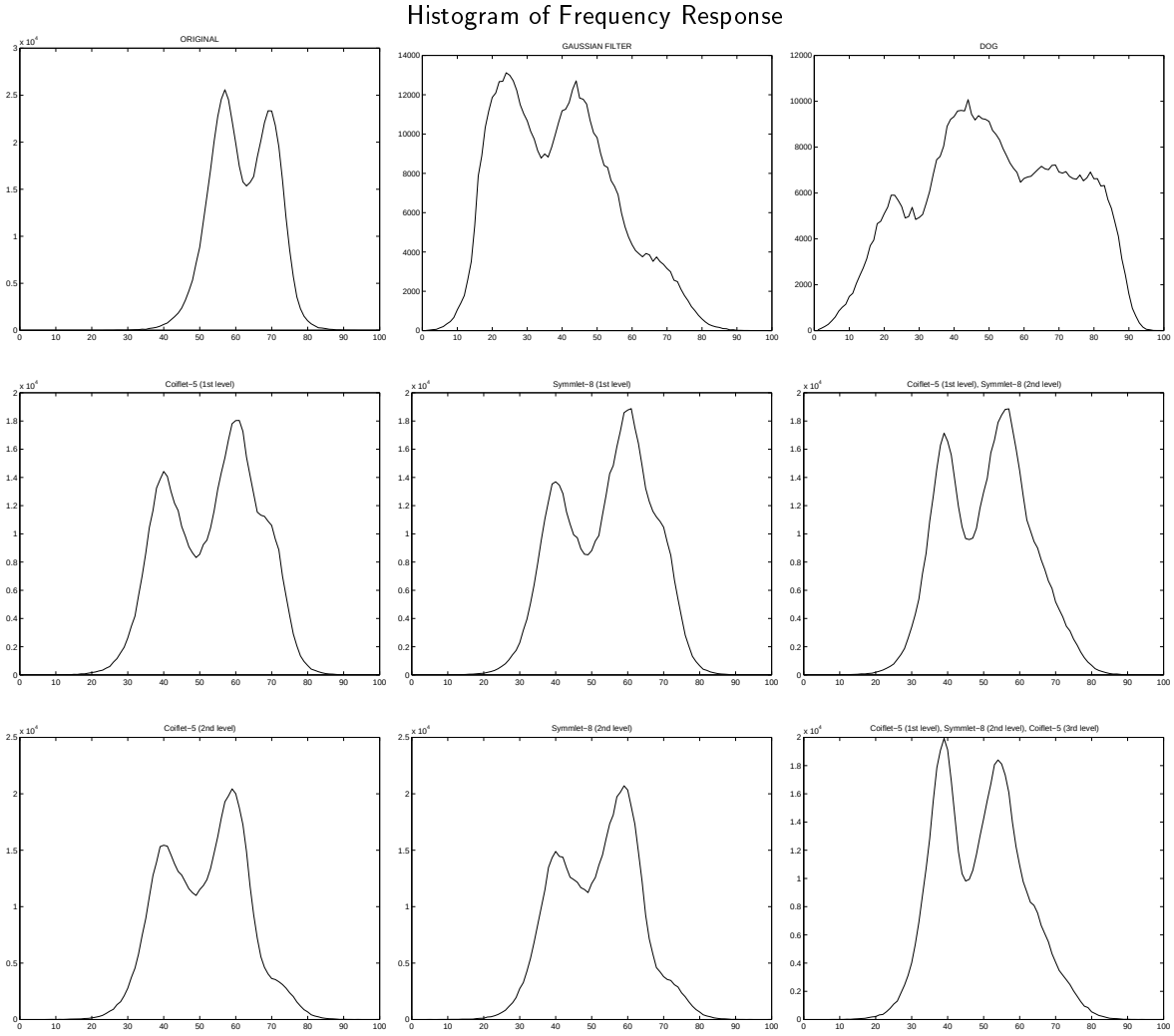


Figure 4: Histogram of the log of the frequency response of different denoising methods. It is evident that the DOG and Gaussian filters distort the histogram while the other denoising methods retain a relatively similar response histogram.

highlight and its shadow, while eliminating high frequency noise. This task is difficult, since a denoising scheme which is generally a low-pass filter that tends to smear edges, and thus, to smear the edges. For a given false positive response, smearing these edges increases the false negative response, namely the undetected mines. The matched filter mask (Figure 5) contains four distinct regions: pre-target, highlight, dead zone and shadow/post-target. It is defined as:

$$I_m(i,j) = \sum_{k=-N_1}^{N_2} \sum_{l=-M_1}^{M_2} g\Big(h(k,l), I_n(i+k, j+l)\Big),$$

where (it is assumed that the input image to the matched filter is normalized so that the average background level is 1.)

$$g\Big(h(k,l), I\Big) = \begin{cases} h(k,l)(I-1) & \text{for } h(k,l) \text{ in the shadow, highlight, and dead zone regions} \\ h(k,l)|I-1| & \text{for } h(k,l) \text{ in the pre-target and post-target regions.} \end{cases}$$

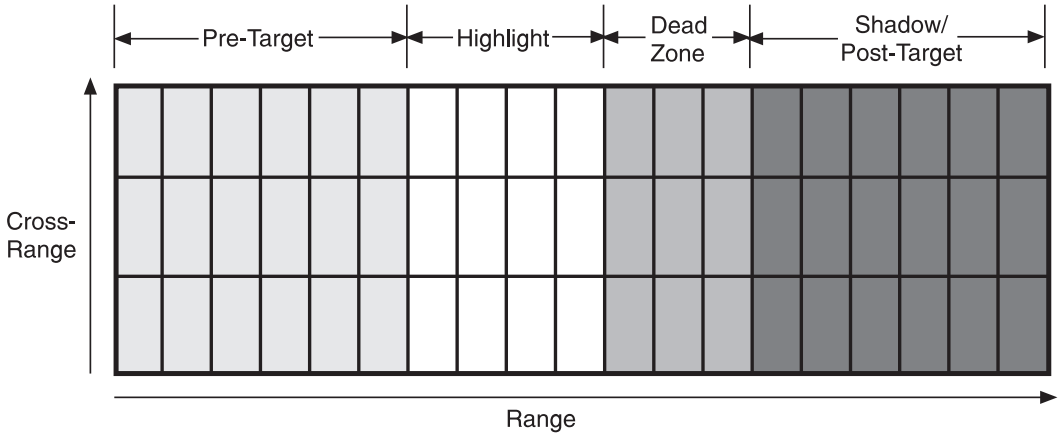


Figure 5: Target signature map of the matched filter.

In each of the four regions, the matched filter coefficients are constant and defined by,

$$h(k,l) = \begin{cases} 1/(S_a(S_o-1)) & \text{shadow region or post-target region} \\ 1/(H_a(H_o-1)) & \text{highlight region} \\ 0 & \text{dead zone region} \\ -1/(T_a|T_o-1|) & \text{pre-target and post-target regions} \end{cases}$$

where,

$$\begin{array}{lcl} S_a & = & \text{area of shadow region in square pixels} \\ S_o & = & \text{reference shadow level} \\ H_a & = & \text{area of highlight region in square pixels} \\ H_o & = & \text{reference highlight level} \\ T_a & = & \text{area of pretarget region in square pixels} \\ T_o & = & \text{reference anomalous background} \end{array}$$

This match filter response is normalized by removing its range-dependent mean and dividing by the standard deviation. To gain better understanding of the effect of the different denoising methods, we study the histogram of the matched filtered images. Figures 6 show these histograms for the original image (top), and for the same image denoised with different techniques. The x-axis corresponds to the intensity of the pixel, the y-axis gives the log of the number of pixels having that intensity. The most important part in these histograms is the behavior at high matched filter responses (the far right part). The longer the tail, the higher the response of the matched filter, while the hight of this tail gives an indication to the possible number of false positives.

## 6. RESULTS

Table 1 shows the performance of the detection stage of the AMDAC algorithm for the different denoising we adopted. It appears that wavelet denoising can increase the number of correct detections, keeping the number of false alarms per image reasonably low. The improvement is around 6% which corresponds to the detection of two mine-like targets formerly missed by the detection algorithm. The Gaussian filter could not improve the performance of the detection algorithm. On the contrary, it increased the number of false alarms per image. In table 1 we do not report the results for the DOG filter. The reason is that the performance of the detection program on the DOG filtered images was too poor, the number of false alarms per image being too large.

It is quite difficult to infer the quality of the various denoising methods from the denoised images (Figure 1). It is however, evident that wavelet based denoising tends to pop up the highlights of the mine-like targets (Figure 1 center).

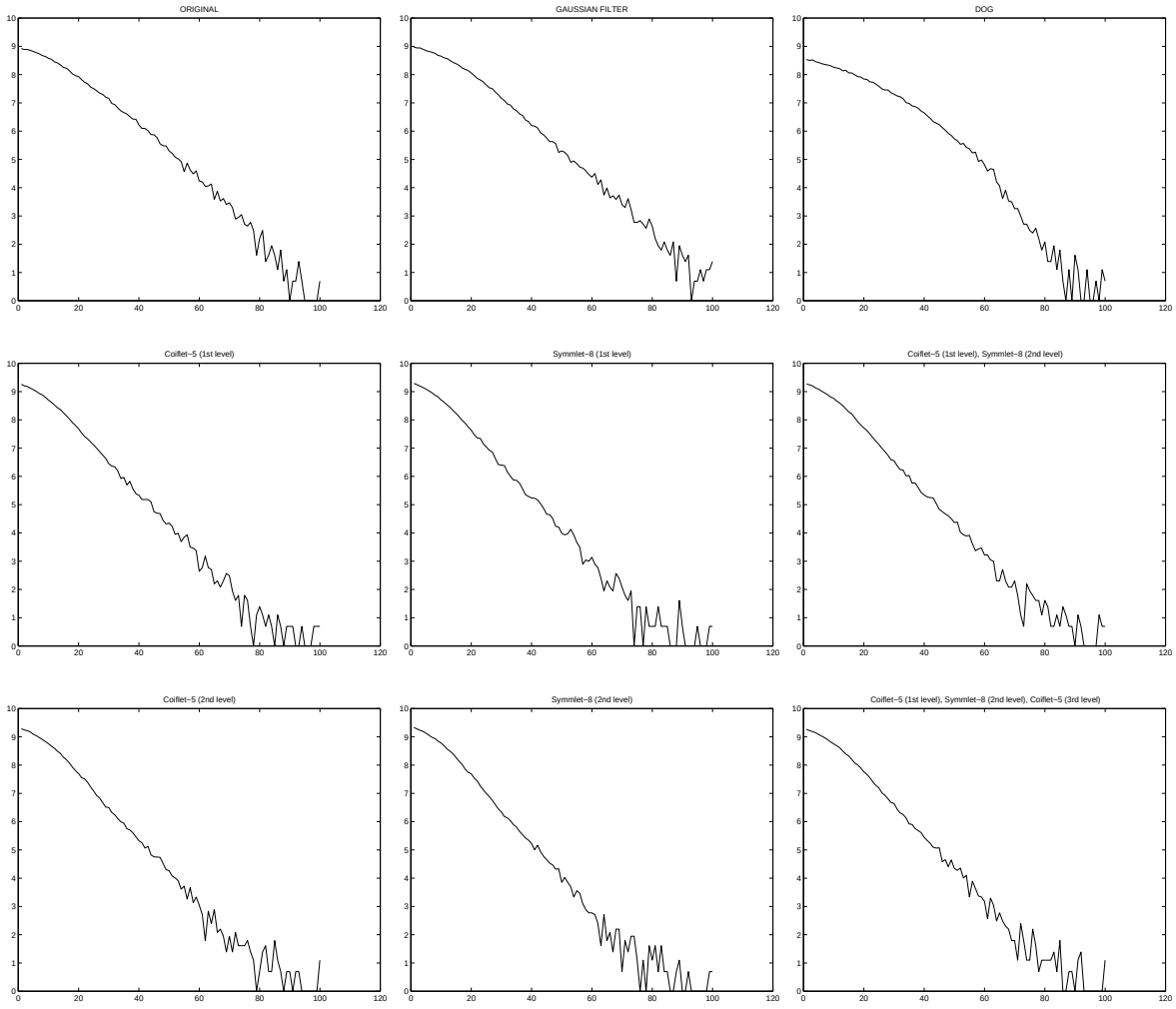


Figure 6: Histogram of the matched filtered image for the original image (top left), and for the same image denoised with different techniques. All graphics are in semilogarithmic scale.

The frequency response of all the denoising methods we tested, apart from the DOG filter, is qualitatively the same. All of them act on the image reducing the values of high frequency coefficients. Thus, the difference in their performance is not directly linked to their frequency response but to their ability to retain higher order structure.

The matched filtered histograms show that there is indeed a difference in the way denoising is performed. As can be seen in Figures 6, images denoised using a wavelet based technique present a shorter tail. This means that the number of high value pixels in the matched filtered image is lower. Since detections are concentrated in this region, this results in a lower number of false alarms per image. On the other hand, both the Gaussian filtered and the DOG filtered images present a tail comparable to that of the original one.

A further interpretation of the different performance is that, using a convolution filter to denoise the image, we modify the shape of the mine-like targets as well. Thus, the matched filter in the detection program is no longer optimal. On the contrary, wavelet denoising projects the image over an orthonormal basis and shrinks only the coefficients corresponding to wavelets whose support is of the same order of the mine-like targets. This does not affect the shape of the targets.

In our analysis we noticed that the performance does not depend on the type of mother wavelet used. Coiflet-5 and Symmlet-8 gave comparable results when the shrinking was applied to the same level. The performance is mostly affected by the choice of the level. That makes sense, since it is equivalent to choosing

the scale at which the noise is present. The best results were obtained when the second level was shrinked. So far, we have not seen an effect to the use of different wavelets at different levels.

## 7. ACKNOWLEDGEMENTS

This work is supported by the Office of Naval Research (code 311).

## 8. REFERENCES

1. D. L. Donoho, "De-noising by Soft-Thresholding", *IEEE Transactions on Information Theory*, **41(3)**, pp. 613–627, 1995.

2. R. R. Coifman and F. Majid, "Adapted waveform analysis", *Progress in Wavelet Analysis and Applications (Proceedings of the International Conference "Wavelets and Applications", Toulouse, France, June, 1992)*, Y. Meyer and S. Roques, pp. 63–76. Editions Frontieres, B.P. 33, 91192 Gif-sur-Yvette, Cedex, France, 1993.

3. G. J. Dobeck and J.C. Hyland, "Sea Mine Detection and Classification Using Side-Looking Sonars", *Proceedings of the SPIE Annual International Symposium on Aerospace/Defense Sensing, Simulation and Control*, **2496**, pp. 442–453, 1995.